MISSING POWER VS LOW-ℓ ALIGNMENTS IN THE COSMIC MICROWAVE BACKGROUND: NO CORRELATION IN THE STANDARD COSMOLOGICAL MODEL

Devdeep Sarkar[1], Dragan Huterer[1], Craig Copi[2], Glenn Starkman[2], Dominik Schwarz[3]

[1] Department of Physics, University of Michigan, 450 Church St, Ann Arbor, MI 48109, USA
[2] CERCA/Department of Physics, Case Western Reserve University, Cleveland, OH 44106-7079, USA
[3] Fakultät für Physik, Universität Bielefeld, Postfach 100131, D-33501 Bielefeld, Germany
(Dated: May 12, 2010)
Draft version May 12, 2010

ABSTRACT

On large angular scales ($\gtrsim 60°$), the two-point angular correlation function of the temperature of the cosmic microwave background (CMB), as measured (outside of the plane of the Galaxy) by the *Wilkinson Microwave Anisotropy Probe*, shows significantly lower large-angle correlations than expected from the standard inflationary cosmological model. Furthermore, when derived from the full CMB sky, the two lowest cosmologically interesting multipoles, the quadrupole ($\ell = 2$) and the octopole ($\ell = 3$), are unexpectedly aligned with each other. Using randomly generated full-sky and cut-sky maps, we investigate whether these anomalies are correlated at a statistically significant level. We conclusively demonstrate that, assuming Gaussian random and statistically isotropic CMB anisotropies, there is no statistically significant correlation between the missing power on large angular scales in the CMB and the alignment of the $\ell = 2$ and $\ell = 3$ multipoles. The chance to measure the sky with both such a lack of large-angle correlation and such an alignment of the low multipoles is thus quantified to be below 10^{-6}.

Subject headings:

1. INTRODUCTION

Several anomalies in the cosmic microwave background maps observed by the WMAP satellite (Bennett et al. 2003; Jarosik et al. 2010) have been recently observed and much discussed in the literature. These include alignments of the lowest modes of CMB anisotropy with each other, and with geometry and direction of motion of the Solar System, as well as unusually low power at these largest scales. Attempts to explain these anomalies include astrophysical, instrumental, cosmological causes, as well as arguments that faulty data analysis or *a posteriori* statistics are at work (for a review, see Copi, Huterer, Schwarz, & Starkman (2010)). Two particularly puzzling features at large angular scales are the alignments of large-angle anisotropies (de Oliveira-Costa, Tegmark, Zaldarriaga, & Hamilton 2004; Schwarz, Starkman, Huterer, & Copi 2004; Land & Magueijo 2005; Copi, Huterer, Schwarz, & Starkman 2006), and the low power at large scales (Spergel et al. 2003; Copi, Huterer, Schwarz, & Starkman 2007); each of these anomalies are $\ll 1\%$ likely. For reviews with differing points of view see Bennett et al. (2010); Copi et al. (2010).

A natural question that arises is whether the alignments and low power at large scales are correlated. Naively, the answer is negative, since the alignments are defined by orientation of the multipoles, and are independent of the total power. In the language of multipole vectors, the normalization at each multipole defines power, and is independent of the multipole vectors that define orientations of multipoles. Such a conclusion has been verified, for full sky maps, by Rakić & Schwarz (2007).

However, the answer for the *cut-sky* maps is less clear *a priori*. Consider the case where the large-scale multipoles are largely planar (as is the case for our own quadrupole and octopole), thus creating alignments. If the sky cut happens to be parallel to this plane, then the cut-sky power may be unusually low, and this may well be happening more often than when the cut is applied to unaligned (statistically isotropic) maps. Clearly, the only safe way to investigate the correlation between the low power and alignments in the presence of the realistic sky cut is to perform Monte Carlo comparisons with Gaussian random, statistically isotropic maps.

In this *Letter* we investigate the correlation between the alignments and low power for the cut-sky as well as full-sky maps assuming a Gaussian random, statistically isotropic, cosmological model.

2. LARGE-SCALE ANOMALIES AND WMAP7

2.1. *Low Power on Large Angular Scales*

The temperature anisotropy in the $\hat{\mathbf{e}}\,[= (\theta, \phi)]$ direction of the microwave sky can be represented by a real scalar function $(\Delta T(\theta, \phi))$ on a sphere, expanded in terms of the multipole moments

$$\Delta T(\hat{\mathbf{e}}) \equiv \Delta T(\theta, \phi) = \sum_{\ell=0}^{\infty} T_\ell(\theta, \phi), \qquad (1)$$

where the ℓth multipole, $T_\ell(\theta, \phi)$, is expressed in terms of the spherical harmonics, $Y_{\ell m}(\theta, \phi)$, as

$$T_\ell(\theta, \phi) = \sum_{m=-\ell}^{\ell} a_{\ell m} Y_{\ell m}(\theta, \phi). \qquad (2)$$

The standard inflationary cosmological model predicts that the fluctuations in the microwave sky can be thought of as being sampled from a statistically isotropic, Gaussian random field of zero mean. Gaussianity dictates that the variances of these $a_{\ell m}$ would fully characterize the distribution and statistical isotropy implies that these variances would depend only on ℓ, allowing us

to write the *ensemble* average of any pair of $a_{\ell m}$ as $\langle a_{\ell m} a^*_{\ell' m'} \rangle = C_\ell \delta_{\ell \ell'} \delta_{mm'}$, where C_ℓ is the (ensemble average of) power in the ℓth multipole. In practice, it is not possible to measure such an ensemble average as we have only one realization of the universe. Instead, one uses its observable estimator, $\hat{C}_\ell$, defined as

$$\hat{C}_\ell \equiv \frac{1}{2\ell+1} \sum_{m=-\ell}^{\ell} |a_{\ell m}|^2. \qquad (3)$$

In the case of statistical isotropy, this $\hat{C}_\ell$, known as the angular power spectrum, is an unbiased estimator of C_ℓ. Additionally, if one assumes Gaussianity, $\hat{C}_\ell$ is the best estimator of C_ℓ with cosmic variance: $\mathrm{Var}(\hat{C}_\ell) = 2\hat{C}_\ell^2/(2\ell+1)$.

Instead of calculating the power in each multipole, one can consider the (real space) two-point angular correlation function of the CMB temperature fluctuations. Assuming statistical isotropy, one can express the angular correlation function as $\mathcal{C}(\hat{\mathbf{e}}_1, \hat{\mathbf{e}}_2) = \mathcal{C}(\theta) \equiv \langle T(\hat{\mathbf{e}}_1) T(\hat{\mathbf{e}}_2) \rangle_\theta$, where $\langle \cdot \rangle_\theta$ represents an ensemble average over the temperatures $T(\hat{\mathbf{e}}_1)$ and $T(\hat{\mathbf{e}}_2)$ in all pairs of directions $\hat{\mathbf{e}}_1$ and $\hat{\mathbf{e}}_2$ separated by the angle θ. One can get an unbiased estimator of $\mathcal{C}(\theta)$ by replacing the ensemble average with the sky average

$$\hat{\mathcal{C}}(\theta) \equiv \overline{T(\hat{\mathbf{e}}_1) T(\hat{\mathbf{e}}_2)}_\theta. \qquad (4)$$

Note that $\hat{C}_\ell$ and $\hat{\mathcal{C}}(\theta)$ only contain precisely the same information for full-sky data, and their analogues in the ensemble are informationally equivalent only if the sky is statistically isotropic. Thus, simultaneous measurements of both $\hat{C}_\ell$ and $\hat{\mathcal{C}}(\theta)$ can be used to probe the validity of the assumption of statistical isotropy.

The two-point angular correlation function, $\hat{\mathcal{C}}(\theta)$, can be directly measured as there is a very large number of independently measured pixels on the WMAP sky. In Fig. 1 we show $\hat{\mathcal{C}}(\theta) \equiv \overline{T(\hat{\mathbf{e}}_1) T(\hat{\mathbf{e}}_2)}_\theta$ (computed in pixel space, using SpICE (Szapudi, Prunet, & Colombi 2001) at NSIDE=512) for the WMAP 7-year coadded data. The results are shown for four different maps of WMAP7: the V and W bands masked with the 7-year KQ75 mask (KQ75y7; henceforth), the ILC map (which covers the full sky), and the cut-sky version of the ILC map (using the same mask). For comparison, we also show the full-sky ILC from the 5-year data. Finally, we show the angular two-point correlation function for the best-fit ΛCDM model for WMAP7 data, along with the 1σ cosmic variance band (in blue) around the best-fit. The most striking feature of $\hat{\mathcal{C}}(\theta)$ for all the cut-sky maps is that they are very close to zero for $\theta \gtrsim 60°$, except for some anti-correlation near $180°$.

To quantify this lack of correlation, we follow past work (Spergel et al. 2003; Copi et al. 2007; Copi, Huterer, Schwarz, & Starkman 2009) and adopt the $S_{1/2}$ statistic to test the total amount of correlation at angles above $60°$:

$$S_{1/2} \equiv \int_{-1}^{1/2} \left[\hat{\mathcal{C}}(\theta) \right]^2 \mathrm{d}(\cos\theta). \qquad (5)$$

The calculation of $S_{1/2}$ using Eq. (5) is susceptible to small-scale fluctuations in $\hat{\mathcal{C}}(\theta)$. To avoid this we evaluate
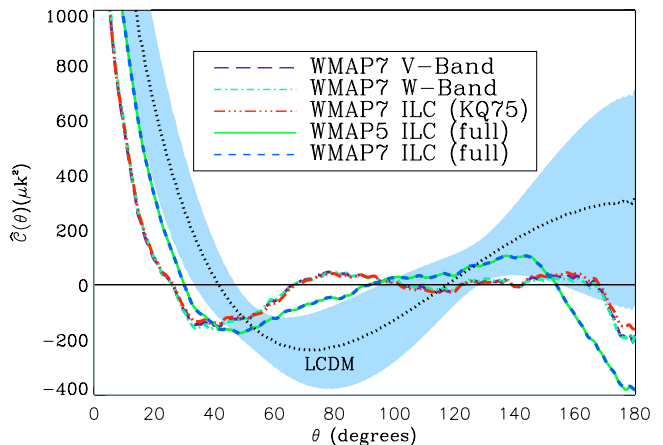

Fig. 1.— The two point angular correlation function from the WMAP 7-year coadded data. The long-dashed and the dot-dashed lines show $\hat{\mathcal{C}}(\theta) \equiv \overline{T(\hat{\mathbf{e}}_1) T(\hat{\mathbf{e}}_2)}_\theta$ for the V and W bands, respectively, both masked with the KQ75y7 mask. The dashed line shows the correlation function for the ILC7 map (which covers the full sky). The solid line shows the same for ILC5 for comparison. The $\hat{\mathcal{C}}(\theta)$ for the cut-sky version of the ILC7 map (using the same mask) is shown by the dot-dot-dot-dashed line. Finally, we show the angular two-point correlation function for the best-fit ΛCDM model with the dotted line, the 1σ cosmic variance band around the best-fit being shown in blue.

$S_{1/2}$ via (Copi et al. 2009)

$$S_{1/2} = \frac{1}{(4\pi)^2} \sum_{\ell,\ell'} (2\ell+1)(2\ell'+1) \hat{\mathcal{C}}_\ell I_{\ell,\ell'}(1/2) \hat{\mathcal{C}}_{\ell'}, \qquad (6)$$

where $I_{\ell,\ell'}(x) = \int_{-1}^{x} P_\ell(x') P_{\ell'}(x') dx'$ and $\hat{\mathcal{C}}_\ell$ is the Legendre transform of $\hat{\mathcal{C}}(\theta)$

$$\hat{\mathcal{C}}_\ell \equiv 2\pi \int_{-1}^{1} P_\ell(\cos\theta) \hat{\mathcal{C}}(\theta) \mathrm{d}(\cos\theta). \qquad (7)$$

The $S_{1/2}$ values, calculated using Eq. (6), for different bands of WMAP 7-year (as well as 5-year, for comparison) coadded data is shown in Table 1. Here we make use of SpICE at NSIDE=64.

2.2. *The Quadrupole-Octopole Alignment*

To measure the level of alignments between the quadrupole and octopole, we use two of the most commonly used statistics: one based on the multipole vectors, and one based on the angular momentum operator. As expected, the two statistics are mutually highly correlated (see Table 2 below); we include both for completeness.

Instead of expanding the temperature anisotropy of the microwave sky in spherical harmonics, one can uniquely describe the temperature anisotropy in the $\hat{\mathbf{e}} [= (\theta, \phi)]$ direction as (Copi, Huterer, & Starkman 2004)

$$T_\ell(\theta, \phi) = A^{(\ell)} \left[\prod_{i=1}^{\ell} \left(\hat{\mathbf{v}}^{(\ell,i)} \cdot \hat{\mathbf{e}} \right) - \mathcal{T}_\ell \right], \qquad (8)$$

where $A^{(\ell)}$ is a scalar which depends only on the total power in the ℓth multipole and $\{ \hat{\mathbf{v}}^{(\ell,i)} | i = 1, ..., \ell \}$ are ℓ 'headless' unit vectors, known as the "multipole vectors". Here $\mathcal{T}_\ell$ is the sum of all possible traces of the first term in the right hand side of the Eq. (8).

3

TABLE 1
$S_{1/2}$-statistic from WMAP 5-year and WMAP 7-year Data

Data Source	V5 (KQ75y5)	W5 (KQ75y5)	ILC5 (KQ75y5)	ILC5	V7 (KQ75y7)	W7 (KQ75y7)	ILC7 (KQ75y7)	ILC7	Theory5 C_ℓ	Theory7 C_ℓ
$S_{1/2}$ (μK^4)	1242	1236	1054	8600	1312	1231	1141	8484	49040	46610

Note: The values of the $S_{1/2}$-statistic are calculated for different bands of WMAP 5-year and WMAP 7-year coadded data. We have used SpICE (Szapudi et al. 2001) at NSIDE=64 and calculated $S_{1/2}$ using Eq. (6) with $\ell_{max} = 30$. The values of $S_{1/2}$ calculated from the best-fit theory C_ℓ are also included for reference.

To test the planarity of the quadrupole and octopole, for each multipole ℓ we form the $\ell(\ell-1)/2$ cross-products (the "oriented area" vectors (Schwarz et al. 2004))

$$\mathbf{w}^{(\ell;i,j)} = \hat{\mathbf{v}}^{(\ell,i)} \times \hat{\mathbf{v}}^{(\ell,j)}, \qquad (9)$$

where the overall signs of the area vectors, $\mathbf{w}^{(\ell;i,j)}$, are unimportant. For the following discussion, let us consider the lone area vector for the quadrupole, $\mathbf{w}^{(2;1,2)}$, and the three area vectors for the octopole: $\mathbf{w}^{(3;1,2)}$, $\mathbf{w}^{(3;2,3)}$, and $\mathbf{w}^{(3;3,1)}$.

To investigate the relative orientation of the quadrupolar plane with the three octopolar planes, we can evaluate the magnitudes of the dot products between $\mathbf{w}^{(2;1,2)}$ and $\mathbf{w}^{(3;i,j)}$, given by

$$A_{1 \{or 2 or 3\}} \equiv \left| \mathbf{w}^{(2;1,2)} \cdot \mathbf{w}^{(3;1,2) \{or (3;2,3) or (3;3,1)\}} \right|. \qquad (10)$$

High values of A_i imply that the $\ell = 2$ and $\ell = 3$ planes are aligned with each other. One can test the combined planarity of the quadrupole and octopole by using the statistic that takes the average of the dot products

$$S^{(3,q)} \equiv \frac{1}{q} \sum_{i=1}^{q} A_i. \qquad (11)$$

Using ILC7 and ILC5, we find $S^{(3,3)} = 0.736$ and $S^{(3,3)} = 0.753$, respectively. In the subsequent sections, to be conservative, we use $S^{(3,3)} = 0.798$ (Copi et al. 2007), obtained using the cleaned full sky map of Tegmark, de Oliveira-Costa, & Hamilton (2003) (TOH; henceforth).

An alternative statistic that tests the planarity is given by the angular momentum dispersion (de Oliveira-Costa et al. (2004)). For each ℓ, an axis $\hat{\mathbf{n}}_\ell$ can be found, around which the angular momentum dispersion

$$\langle T_\ell(\hat{\mathbf{n}}_\ell)|(\hat{\mathbf{n}}_\ell \cdot \mathbf{L})^2|T_\ell(\hat{\mathbf{n}}_\ell)\rangle = \sum_{m=-\ell}^{\ell} m^2 |a_{\ell m}(\hat{\mathbf{n}}_\ell)|^2 \qquad (12)$$

is maximized. Here $\mathbf{L}$ is the angular momentum operator and $a_{\ell m}(\hat{\mathbf{n}}_\ell)$ are the spherical harmonic coefficients of the CMB map in coordinate system with its z-axis in the $\hat{\mathbf{n}}_\ell$ direction. Note that this angular momentum axis distills a limited amount of information from each multipole, reducing the d.o.f. to just 2 from the 2ℓ d.o.f. in $\hat{\mathbf{v}}^{(\ell,i)}$.

Copi et al. (2006) found that $\hat{\mathbf{n}}_2 \cdot \hat{\mathbf{n}}_3 = 0.962$ for the TOH map. The corresponding values obtained from the analysis of the WMAP 7-year data is 0.937. The measured values of $S^{(3,3)}$ and $\hat{\mathbf{n}}_2 \cdot \hat{\mathbf{n}}_3$ consistently indicate that the quadrupole and the octopole are unexpectedly aligned, both in the 5 and 7 year WMAP data.

3. IN SEARCH FOR A CORRELATION

We have just seen that WMAP7 confirms results from its earlier data releases: at large angular scales ($\gtrsim 60°$), the two-point correlation function of the temperature of the CMB, as measured by WMAP, is significantly smaller in magnitude than expected from the predictions of the standard inflationary cosmological model; and in addition, the planes of the quadrupole ($\ell = 2$) and the octopole ($\ell = 3$) are unexpectedly aligned with each other. In this section, we investigate whether these anomalies are correlated at a statistically significant level.

More specifically, we want to investigate a couple of different scenarios:

- If the Gaussian random, statistically isotropic CMB maps are constrained to have low angular correlation on large angular scales, are they more likely to exhibit planarity and alignment of the quadrupole and octopole?

- If the Gaussian random, statistically isotropic CMB maps are constrained to have aligned quadrupole and octopole, are they more likely to have low angular correlation on large angular scales?

Although the answers to the above questions might seem to be obvious for the full-sky case, there is no direct reason why no such correlation should exist for the case of cut-sky maps. In what follows, we attempt to address each of these questions for both the full-sky and the cut-sky cases.

3.1. Monte-Carlo Analysis

We first generate 100,000 constrained (low angular correlation on large angular scales) realizations of the CMB sky with selection criterion of $S_{1/2} < 8583(\mu K)^4$ (i.e. lower than the ILC5 full-sky $S_{1/2}$ from Copi et al. (2009)) *and* the cut-sky $S_{1/2} < 1152(\mu K)^4$ (i.e. lower than the ILC5 cut-sky map).[1] This is our sample of Gaussian random, statistically isotropic maps that are constrained to have low angular correlation on large scales, and we use them to test the probability of alignments under this constraint, i.e., the probability of having $S^{(3,3)} > 0.798$ for these low-correlation maps. We also calculate the probability of these low–correlation maps to have aligned angular momentum dispersion axes, i.e., $\hat{\mathbf{n}}_2 \cdot \hat{\mathbf{n}}_3 > 0.962$. We

---

[1] It should be noted that these values of $S_{1/2}$ are corresponding to the WMAP 5-year ILC full sky (DQ corrected) and WMAP 5-year ILC cut sky (using KQ75y5 mask, DQ corrected) maps, since we started this analysis prior to WMAP 7-year data release. In fact, these values are comparable to the corresponding values for the WMAP 7-year results shown in Table 1.

TABLE 2
PROBABILITIES OF HAVING LOW-POWER ON LARGE ANGULAR
SCALES AND QUADRUPOLE-OCTOPOLE ALIGNMENT FOR THE
UNCONSTRAINED AND CONSTRAINED MAPS

Probabilities (in %)	Unconstrained Maps	Constrained Maps	
		Low Power	Full-Sky Aligned
$P\left(S_{1/2}^{\text{full sky}}\right)$	7.0	—	**6.9**
$P\left(S_{1/2}^{\text{cut sky}}\right)$	0.05	—	**0.07**
$P\left(S^{(3,3)}\right)$	0.12	**0.12**	—
$P\left(\hat{\mathbf{n}}_2 \cdot \hat{\mathbf{n}}_3\right)$	0.37	**0.36**	**99.6**

Note: The statistics $S^{(3,3)}$ and $\hat{\mathbf{n}}_2 \cdot \hat{\mathbf{n}}_3$ are always evaluated on the full sky. The cases with the dashes denote circular comparisons.

then compare these probabilities with the corresponding ones for the unconstrained maps.

To test the probability of low angular correlation on Gaussian random, statistically isotropic maps that are constrained to be aligned, we generate 100,000 MC maps constrained to have $S^{(3,3)} > 0.798$, calculated using the full sky as the cut sky alignments are extremely difficult to test (the errors in multipole vectors become large for a cut larger than a few degrees). We then evaluate the $S_{1/2}$ statistic for these constrained maps (with and without applying the WMAP 5-year KQ75 mask (KQ75y5)) and calculate the percentage of these maps having $S_{1/2} < 8583(\mu K)^4$ (for the full-sky case) or $S_{1/2} < 1152(\mu K)^4$ (for the case using KQ75y5). We also calculate the probability of these constrained maps to have $\hat{\mathbf{n}}_2 \cdot \hat{\mathbf{n}}_3 > 0.962$. As discussed before, we then compare these probabilities with the corresponding ones for the unconstrained maps.

3.2. Results and Discussions

Our main results are summarized in Table 2. Using our sample of 100,000 low-power maps, we find the probability of these maps to have $S^{(3,3)} > 0.798$ is 0.12%, which is the same as the probability of completely unconstrained maps to have quadrupole-octopole alignment (Copi et al. 2006). This shows that the low-power maps do not have a higher probability to have an alignment of the $\ell = 2$ and $\ell = 3$ planes. The probability of these low-power maps to have aligned angular momentum dispersion axes ($\hat{\mathbf{n}}_2 \cdot \hat{\mathbf{n}}_3 > 0.962$) is also very low (0.36%) and essentially identical as that found for unconstrained maps (0.37%; Copi et al. (2006)).

Using 100,000 maps constrained to be have quadrupole-octopole alignment ($S^{(3,3)} > 0.798$), we find 6.9% probability for these maps to have $S_{1/2} < 8583(\mu K)^4$ for the full-sky case. Comparing

this with the probability (7.0%) of having low angular correlation for completely unconstrained maps, we find no correlation between alignment and low angular correlation for the full-sky case.

For the cut-sky case (using the KQ75 mask), however, we find 0.07% probability for these maps to have $S_{1/2} < 1152(\mu K)^4$. This probability is slightly higher ($\gtrsim 2\sigma$ with σ a Poisson error) than $P\left(S_{1/2}^{\text{cut sky}}\right) = 0.05\%$ for unconstrained maps. However, this difference is not statistically significant to conclude any detectable correlation between alignment and low power for cut skies.

4. CONCLUSION

Applying the multipole vector formalism to Gaussian random and statistically isotropic realizations of CMB maps (both full-sky and cut-sky) lacking correlation on large angular scales, we find no increased probability for alignment of the quadrupole and the octopole than expected in the case of unconstrained random maps. These low-power maps also do not show higher angular momentum dispersion. On the flip side, we also find that realizations of CMB maps (both full-sky and cut-sky), constrained to have aligned quadrupole and octopole at a level greater than that exhibited by WMAP, do not have lower power on large scales than expected in the case of unconstrained random realizations.

Our results conclusively demonstrate that, under the standard Gaussian and isotropic model, there is no statistically significant correlation between the missing power on large angular scales in the CMB and the alignment of the $\ell = 2$ and $\ell = 3$ multipoles. Therefore, in the context of the standard model, their combined statistical significance is equal to the product of their individual significances. For example, simultaneous observation of the missing large-angle correlations with probability $P(S_{1/2}^{\text{cut sky}}) \lesssim 0.1\%$ and alignments with the probability $P(S^{(3,3)}) \simeq 0.1\%$ is likely at the $\lesssim 0.0001\%$ level. Given that both anomalies occur at the largest observable scales and are correlated with special directions in the sky (ecliptic and/or dipole), they clearly require a causal explanation.

REFERENCES

Bennett, C. L., et al. 2003, ApJS, 148, 1
Bennett, C. L., et al. 2010, arXiv:1001.4758
Copi, C. J., Huterer, D., Schwarz, D. J., & Starkman, G. D. 2006, Mon. Not. Roy. Astron. Soc., 367, 79
Copi, C. J., Huterer, D., Schwarz, D. J., & Starkman, G. D. 2007, Phys. Rev. D, 75, 023507
—. 2009, MNRAS, 399, 295
Copi, C. J., Huterer, D., Schwarz, D. J., & Starkman, G. D. 2010, Advances in Astronomy
Copi, C. J., Huterer, D., & Starkman, G. D. 2004, Phys. Rev., D70, 043515
de Oliveira-Costa, A., Tegmark, M., Zaldarriaga, M., & Hamilton, A. 2004, Phys. Rev., D69, 063516

Jarosik, N., et al. 2010, arXiv:1001.4744
Land, K., & Magueijo, J. 2005, Phys. Rev. Lett., 95, 071301
Rakić, A., & Schwarz, D. J. 2007, Phys. Rev., D75, 103002
Schwarz, D. J., Starkman, G. D., Huterer, D., & Copi, C. J. 2004, Phys. Rev. Lett., 93, 221301
Spergel, D. N., et al. 2003, ApJS, 148, 175
Szapudi, I., Prunet, S., & Colombi, S. 2001, ApJ, 561, L11
Tegmark, M., de Oliveira-Costa, A., & Hamilton, A. J. 2003, Phys. Rev., D68, 123523